STRUCTURE AND OPTICAL PROPERTIES OF $Zn_{1-x}Ni_xO$ NANOPARTICLES BY COPRECIPITATION METHOD

RUBY CHAUHAN[a,b*], ASHAVANI KUMAR[c], RAM PAL CHAUDHARY[a]
[a]*Department of Chemistry, Sant Longowal Institute of Engg. & Tech. Longowal 148 106 India*
[b]*Technology Education and Research Integrated Institutions, Kurukshetra 136 119 India*
[c]*Department of Physics, National Institute of Technology, Kurukshetra 136 119 India*

Nanocrystals of undoped and nickel doped zinc oxide (Zn_{1-x} Ni $_x$ O, where x = 0.00 to 0.05) were synthesized by coprecipitation method. Crystalline phases and optical absorption of prepared samples were determined by X-ray diffraction and UV-visible spectrophotometer. The average particle size was determined from X-ray line broadening. X-ray study revealed that Ni doped ZnO crystallized in hexagonal wurtzite structure. Doping of ZnO with Ni^{2+} was intended to enhance the surface defects of ZnO. The incorporation of Ni^{2+} in the place of Zn^{2+} provoked an increase in the size of nanocrystals as compared to undoped ZnO. Crystalline size of nanocrystals varied from 10 to 40 nm as the calcinations temperature increased. Enhancement in the optical absorption of Ni doped ZnO indicated that it can be used as an efficient photocatalyst under visible light irradiation. Optical absorption measurements indicated red shift in the absorption band edge upon Ni doping. The band gap value of prepared undoped and nickel doped ZnO nanoparticles decreased as annealing temperature was increased up to 800 ^oC

(Received January 27, 2011; accepted February 23, 2011)

Keywords: Nanoparticles, Coprecipitation, Optical absorption, XRD, UV-vis spectrophotometer.

1. Introduction

Nanocrystalline materials have attracted a wide attention due to their unique properties and immense potential application in nano device fabrication[1-4]. Zinc oxide (ZnO) has a direct wide bandgap (3.4 eV at Room temperature), which is n-type semiconductor. In ambient condition, ZnO has a stable hexagonal wurtzite structure with lattice spacing a = 0.325 nm and c = 0.521 nm and composed of a number of alternating planes with tetrahedrally-coordinated O^{2-} and Zn^{2+} ions, stacked alternately along the c-axis. It has attracted intensive research effort for its unique properties and versatile applications in transparent electronics, ultraviolet (UV) light emitters, piezoelectric devices, chemical sensors and heterogenous photocalysts[5-15]. It has been proposed to be a more promising UV emitting phosphor than GaN because of its larger exciton binding energy (60 meV). All these predominant properties make ZnO a great potential in the field of nanotechnology.

Various chemical methods have been developed to prepare nanoparticles of different materials of interest. Most of the ZnO crystals have been synthesized by traditional high temperature solid state method in which, it is difficult to control the particle properties and also energy consuming. ZnO nanoparticles can be prepared on a large scale at low cost by simple solution based method, such as chemical precipitation, sol-gel synthesis, and hydrothermal reaction[16-21]. Many of the earliest synthesis of nanoparticles were achieved by coprecipitation

*Corresponding author: ashavani@yahoo.com

of sparingly soluble products from aqueous solution followed by thermal decomposition of those products to oxides. Coprecipitation method is a promising alternative synthetic method because of the low process temperature and easy to control the particle size. Some of the most commonly substances used in coprecipitation operations are hydroxides, carbonates, sulphates and oxalates.

In the present work undoped and Ni doped ZnO nanoparticles were synthesized by using chemical coprecipitation method, which is robust and reliable to control the shape and size of particles without requiring the expensive and complex equipments[22].

2. Experimental

All chemicals used were AR grade from Fisher Scientific and used without further purification. X-Ray Diffraction (XRD) patterns were recorded on a Rigaku mini desktop diffractometer using graphite filtered CuK_α radiation ($\lambda = 1.54056\ A^o$) at 40 KV and 100 mA with scanning rate of 3 degree per minute (from $2\theta = 5^o$ to 80^o). Optical absorption spectra were recorded on Shimadzu double beam double monochromator spectrophotometer (UV-2550), equipped with integrated sphere assembly ISR-240A in the range of 190 to 900 nm.

Coprecipitation method (Preparation of undoped and nickel doped zinc oxide nanoparticles)

The starting materials, $ZnSO_4.7H_2O$ and $Ni(NO_3)_2.6H_2O$ solution were prepared as follows: Solution-A: 0.1M $ZnSO_4.7H_2O$ dissolved in distilled water and Solution-B: 0.1M $Ni(NO_3)_2.6H_2O$ in a distilled water. Mixing these solutions has resulted solution C. The experiment was performed at room temperature. Separately, a buffer solution (pH = 4.6) was prepared by dissolving appropriate amounts of sodium hydroxide and sodium carbonate in distilled water. The pH of buffer solution was selected so as to cause precipitation of the nickel carbonate/ basic zinc carbonate from the solution C. The Buffer solution was then added drop wise to the vigorously stirred solution C to produce a green/white, gelatinous nickel carbonate/basic zinc carbonate precipitate. After addition of the reagents, the mixture was stirred for two hours at room temperature. The precipitate was filtered and washed with distilled water. The precipitate was dry at 110°C for two hours and calcinations were performed at 300 °C, 400 ^{o}C, 500 ^{o}C, 800 ^{o}C and 1000 ^{o}C in muffle furnace. The nickel carbonate/ basic zinc carbonate precipitate was decomposed in nickel doped zinc oxide.

The reactions and discussion for obtaining nickel doped zinc oxide are presented below:
Sodium hydroxide precipitates; the white, gelatinous zinc hydroxide:

$$(Zn^{2+} + SO_4^{2-}) + 2(Na^+ + OH^-) \rightarrow Zn(OH)_2 + (2Na^+ + SO_4^{2-})$$

The precipitate is soluble in sodium hydroxide reagent, resulting zincates, which behave like a weak acid:

$$Zn(OH)_2 + 2(Na^+ + OH^-) \rightarrow (2Na^+ + ZnO_2^{2-}) + H_2O$$

Sodium carbonate precipitates with zinc salts; the white basic carbonate with variable composition:

$$4\,(Zn^{2+} + SO_4^{2-}) + 4(\,2Na^+ + CO_3^{2-}) + HOH \rightarrow Zn_4(CO_3)_3(OH)_2 + CO_2 + 4(\,2Na^+ + SO_4^{2-})$$

Decomposition reaction of basic zinc carbonate (hydrozincite) in zinc oxide is written as:

$$Zn_4(CO_3)_3(OH)_2 \rightarrow 4ZnO + H_2O + 3CO_2$$

. Sodium hydroxide precipitates the nickel oxide. Sodium carbonate precipitates the nickel carbonate, which decomposes in nickel oxide. The reactions are written as:

$$(Ni^{2+} + 2\,NO_3^-) + 2(Na^+ + OH^-) \rightarrow NiO + 2(Na^+ + NO_3^-)$$

$$(Ni^{2+} + 2\,NO_3^-) + (2Na^+ + CO_3^{2-}) \rightarrow NiCO_3 + 2(Na^+ + NO_3^-)$$

$$NiCO_3 \rightarrow NiO + CO_2$$

3. Results and discussion

X-ray diffraction studies: Figures 1-(a)&(b) show the XRD diffraction patterns of undoped and nickel doped zinc oxide ($Zn_{1-x}\,Ni_{\,x}\,O$,where x = 0.00 to 0.05) powder samples at 800 and 1000^{o}C temperatures. In our case all the diffraction peaks at angles (2θ) of 31.36, 34.03,

35.86, 47.16, 56.26, 62.54, 67.64, and 68.79 correspond to the reflection from (100), (002), (101), (102), (110), (103), (200), and (112) crystal planes of the hexagonal wurtzite zinc oxide structure. The measured d-spacing of 2.81, 2.60, 2.47, 1.91, 1.62, 1.47, 1.40, 1.37, 1.36, 1.30 and 1.23 A^{o} also correspond to the reflection from (100), (002), (101), (102), (110), (103), (200), and (112) crystal planes of the wurtzite structure. All the diffraction peaks agreed with the reported JCPDS card no. 80-0075. No additional peaks corresponding to the secondary phases of nickel oxides were obtained for x = 0.01 to 0.05 at 800 ^{o}C, which indicates that the wurtzite structure is not disturbed by the Ni substitution. A very small additional peak attributable to secondary phase of nickel oxide was observed for x = 0.01 to 0.05 at 1000 ^{o}C according to JCPDS card no.78-0643. Thus, we can conclude that the doping of Ni does not change the wurtzite structure of ZnO and hence Ni^{2+} substitutes Zn^{2+} site into the crystal lattice.

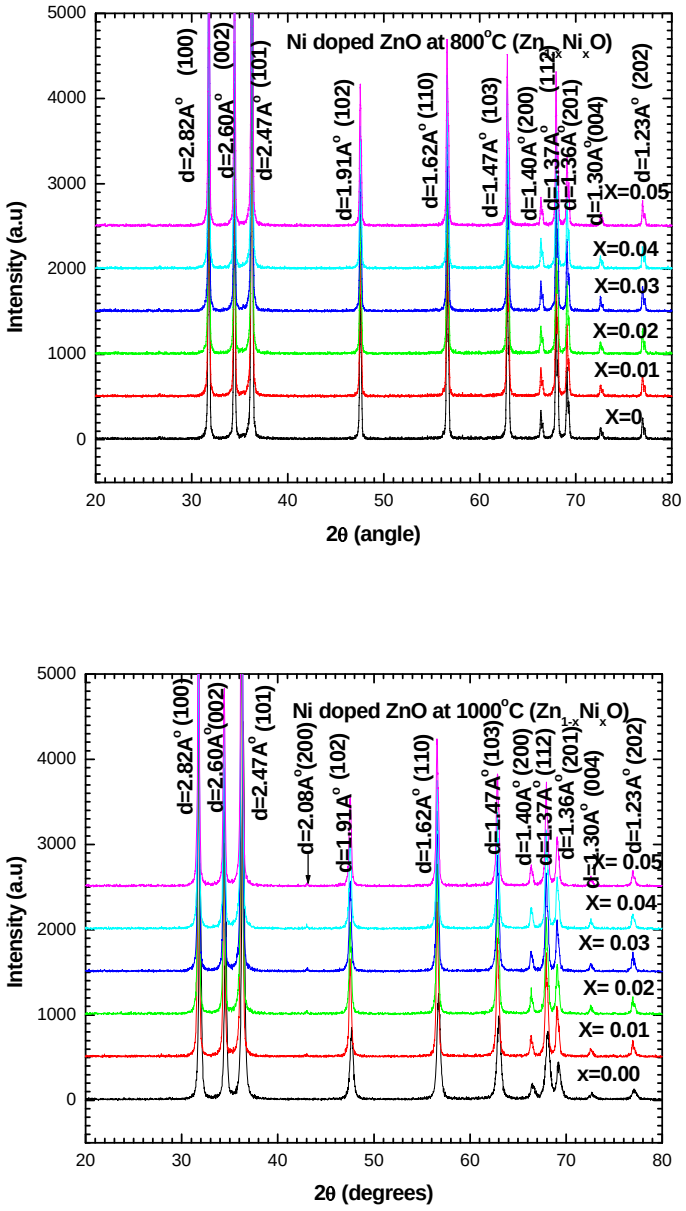

(a) **(b)**

Fig. 1 XRD patterns of Undoped and Ni doped ZnO nanoparticles at (a) 800^{o}C and (b) 1000^{o}C. The arrows indicate the formation of nickel oxides.

A definite line broadening of the diffraction peaks is an indication that the synthesized materials are in nanometer range. It was clearly observed from the XRD patterns that with the increased in temperature of calcinations at 300 to 1000 oC, the diffraction peaks become sharper and stronger; which suggest that the crystal quality of the nanoparticles are improved and the particles sizes are increased. The mean crystalline size was calculated from the full-width at half-maximum (FWHM) of XRD lines by using the Debye-Scherrer formula:

$$D_{h,k,l} = 0.9\lambda / (\beta_{h,k,l}\cos\theta)$$

where D is the average crystalline diameter, λ is the wave-length in angstrom, β is the line width at half–maximum and θ is the Bragg angle. We used the most intense peak (101) in the XRD patterns to calculate the average crystalline size. It can be seen that the average size of nanoparticle increases as the heating temperature is increased and decreases as the doping percentage of nickel metal is increased. This is due to the change of growth rate between the different crystallographic planes. The calculated values of particles size are presented in Table 1 for undoped and Ni doped (1-5%) ZnO at 800 ^{o}C and 1000 ^{o}C. The particles size are in the range of 28 to 37 nm at 800^{o}C and 30 to 42 nm at 1000 ^{o}C corresponding to the $Zn_{1-x}Ni_xO$ (x = 0.0 to 0.05) nanoparticles respectively. The particles size at 500 ^{o}C are about 12 nm for undoped ZnO; while 18 for Ni doped ZnO at 5% doping respectively.

Table 1. Variation of size with temperature of undoped and Ni doped ZnO nanoparticles.

% of doping of Ni	**Average size of particles for sample annealed at temperature 800^{o}C**	**Average size of particles for sample annealed at temperature 1000^{o}C**
0 %	28.0	30.0
1 %	37.0	42.0
2 %	36.0	42.0
3 %	36.0	41.0
4 %	35.0	40.0
5 %	35.0	40.0

Table 2. Variations of Absorption edge with temperature of undoped and Ni doped ZnO nanoparticles.

Temperature ^{o}C	Absorption edge (nm)	
	Undoped ZnO	5% Ni doped ZnO
300	370	387
400	406	420
500	413	427
800	427	435

Table 3. Variations of band gap with temperature of undoped and Ni doped ZnO nanoparticles.

Temperature ^{o}C	Band Gap (eV)	
	Undoped ZnO	5% Ni doped ZnO
300	3.35	3.20
400	3.05	2.95
500	3.00	2.90
800	2.90	2.85

Figure 2 shows the most intense peaks of undoped and nickel doped ZnO, at the doping concentration of 5% and the sintered temperature at 500 ^{o}C. When ZnO doped with Ni^{2+} the peak is moved towards higher angle in comparison to undoped ZnO. This occurs because of the difference between the ionic radii of the elements (rZn^{2+}=0.60 A^{o}, rNi^{2+}=0.55 A^{o})[23] .

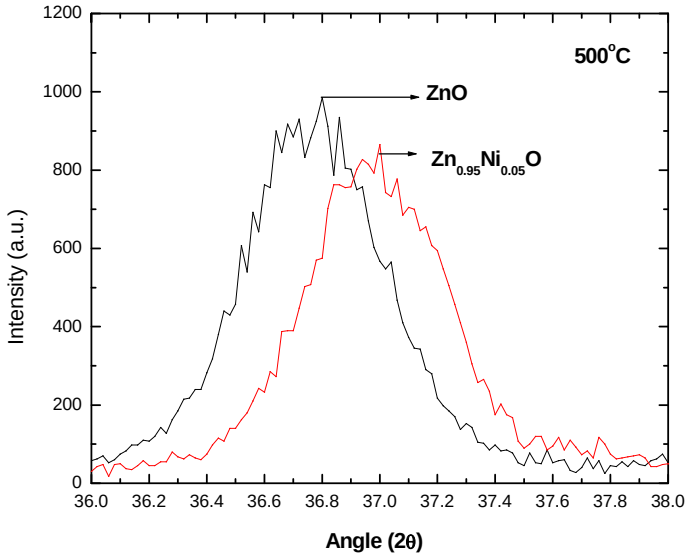

Fig.2 Displacement of the most intense peak of the XRD pattern provoked by the insertion of Ni ions in the crystalline lattice of ZnO.

Optical studies: The optical absorption spectra of undoped and nickel doped zinc oxide ($Zn_{1-x}Ni_xO$ where, x = 0.00, 0.05) samples by UV-vis spectrophotometer in the range of 200 to 800 nm were presented. From figures 3(a) & (b) it can be seen that the excitonic absorption peak of as prepared undoped and nickel doped samples appears around 260 nm which is fairly blue shifted from the absorption edge (i.e much below the band gap wavelength of 365 nm, Eg = 3.4 eV) of bulk ZnO. The excitonic absorption peak of as prepared undoped and nickel doped samples become broad as the temperature increases. The sharp excitonic peak in the absorption spectra at 300 ^{o}C is indicative of the small size distribution of nanocrystal in the samples and broadening of peaks at higher temperatures clearly indicates the increase in size of nanocrystals with the increase of temperatures. It can be observed clearly from figures 3(a) & (b) that the absorbance increases from temperature 300 ^{o}C to 500 ^{o}C but it decreases at the temperature of 800 ^{o}C. In Ni doped ZnO at 500 ^{o}C an absorption band localized between 550 nm and 700 nm corresponding to the spin orbit $^{3}T_1(F) \rightarrow {}^{3}T_1(P)$ ligand field transition of Ni^{2+} in the tetrahedral symmetry is observed for the $Zn_{1-x}Ni_xO$ from that of undoped ZnO sample [24,25]. The energy band gap is determined by using the relationship:

$$\alpha = A\,(h\nu - E_g)^n$$

where hν= Photon energy, α= Absorption coefficient (α = 4πk/λ; k is the absorption index or absorbance, λ is wavelength in nm), E_g =Energy band gap, A=constant , n=1/2 for allowed direct band gap. Exponent n depends on the type of transition and it may have values1/2, 2, 3/2 and 3 corresponding to the allowed direct, allowed indirect, forbidden direct and forbidden indirect transitions respectively [26]. The value of band gap was determined by extrapolating the straight line portion of $(\alpha\ h\nu)^2 = 0$ axis; as shown in figure 4(b) at temperature 400 ^{o}C. The band gap decreases from 3.05 eV to 2.95 eV with Nickel (5 %) doping at temperature 400 ^{o}C. The Absorption edge values of as prepared undoped and nickel doped samples were found to increase with increase in temperature from 300 to 800 ^{o}C but the band gap values of as prepared undoped and nickel doped samples were found to decrease with increase in temperature from 300 to 800 ^{o}C as presented in tables 2 & 3. It is visible from figure 4(a) that in Ni doped ZnO sample the band edge is shifted to lower energy side.

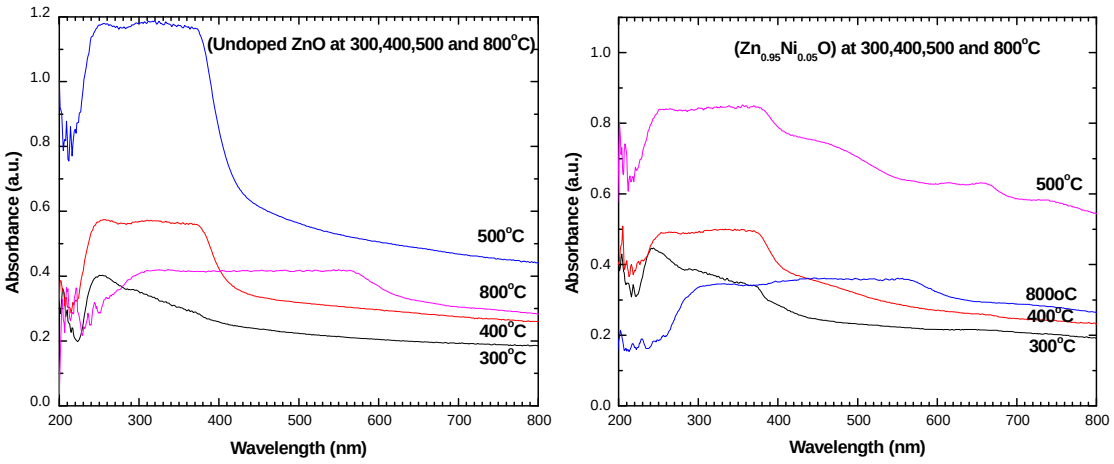

(a) (b)

Fig.3 Optical absorption spectra of (a) undoped ZnO nanoparticles and (b) nickel doped ZnO nanoparticles at 300, 400, 500 and 800°C

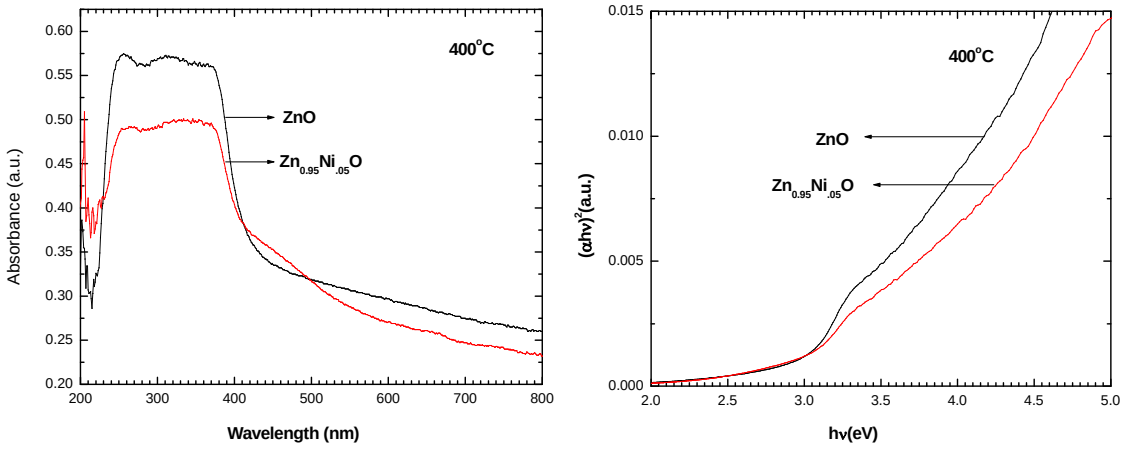

(a) **(b)**

Fig. 4 (a) Optical absorption spectra of undoped and nickel (5%) doped ZnO nanoparticles at 400°C (b) $(\alpha h\nu)^2$ vs. photon energy (hν) for undoped and Nickel doped ZnO samples at 400°C.

4. Conclusions

Nanocrystals of undoped and nickel doped ZnO were successfully synthesized by using a chemical coprecipitation method. The crystalline structure, optical properties and band gap were determined by XRD and UV-visible spectra. XRD analysis shows that the prepared samples are in hexagonal wurtzite phase. The particle size can be adjusted by controlling the reaction temperature. The average size of nanoparticle increases as the heating temperature is increased and decreases as the doping percentage of nickel metal is increased. The strongest absorption peak appears at around 260 nm, which is blue shifted from the absorption edge of bulk ZnO (365 nm). The band gap value of prepared undoped and nickel doped ZnO nanoparticles decreases as annealing temperature increased from 300 to 800 °C. Optical absorption measurements indicate red shift in the absorption band edge upon Ni doping.

Acknowledgements

Authors are thankful to Dr. Sanjeev Aggrawal and Nidhi Sekhawat, Kurukshetra University, Kurukshetra for technical support for getting UV-VIS spectra. We are also thankful to the Director, NIT, Kurukshetra for XRD facilities in physics department.

References

[1] N. Golego, S.A. Studenikin and M. Cocivera, J. Electrochem. Soc., **147**, 1592 (2000).
[2] Y. Lin, Z. Zhang, Z. Tang, F. Yuan and J. Li, Adv. Mater. Opt. Electron**, 9**, 206 (1999).
[3] X. Wang, J. Song, J. Liu and Z.L. Wang, Science, **316**, 102 (2007).
[4] K. Keren, R.S. Berman, E. Buchstab, U. Sivan, E. Braun, Science, **302**, 1380 (2003).
[5] K. Nomura, H. Ohta, K. Ueda, T. Kamiya, M. Hirano, H. Hosono, Science, **300**, 1269 (2003).
[6] T. Nakada, Y. Hirabayashi, T. Tokado, D. Ohmori, T. Mise, Sol. Energy, **77**, 739 (2004).
[7] S. Y. Lee, E. S. Shim, H. S. Kang, S. S. Pang, J. S. Kang, Thin Solid Films, **437**, 31 (2005).
[8] R. Könenkamp, R. C. Word, C. Schlegel, Appl. Phys. Lett., **85**, 6004 (2004).
[9] S. T. Mckinstry, P. Muralt, J. Electroceram., **12**, 7 (2004).
[10] Z. L. Wang, X. Y. Kong, Y. Ding, P. Gao, W. L. Hughes, R. Yang,Y. Zhang, Adv. Funct. Mater., **14**, 943 (2004).
[11] M. S. Wagh, L. A. Patil, T. Seth, D. P. Amalnerkar, Mater. Chem. Phys., **84**, 228 (2004).
[12] Y. Ushio, M. Miyayama, and H. Yanagida, Sensor Actuat., B **17**, 221 (1994).
[13] H. Harima, J. Phys. Condens. Matter., **16**, S5653 (2004).
[14] S. J. Pearton, W. H. Heo, M. Ivill, D. P. Norton, and T. Steiner, Semicond. Sci. Technol., **19**, R59 (2004).
[15] M.A. Garcia, J.M. Merino, E.F. Pinel, A.J. Quesada, D. Venta, M.L.R. Gonza, G.R. Castro, P. Crespo, J. Llopis, J.M.G. Calbet, A.Hernando, Nano letter., **7** , 1489-1494 (2007**)**.
[16] Q.P. Zhong , E. Matijevic, J.Mater. Chem., **3**, 443 (1996).
[17] W. Lingna , M. Mamoun, J.Mater. Chem., **9** , 2871 (1999).
[18] D.W. Bhnemann, C. Kormann, M .R. Hoffmann, J.Phys. Chem., **91** ,3789 (1987).
[19] Z. Hui, Y.Deren, M. Xiangyang, J.Yujie, X. Jin, Nanotechnology., **15** , 622 (2004).
[20] J.Zhang, L. D. Sun, J.L. Yin, Chem.Mater., **14** , 4172 (2002).
[21] W.J. Li, E.W. Shi, Z.W. Yin, J.Mater.Sci.Lett., **20**, 1381 (2001).
[22] A.O. Cadar, C. Roman, L. Gagea, B.A. Matei, I. Cernica, IEEE Xplore., 315 (2007).
[23] S.Ekambaram, J.Alloys compd., **390**, L4-L6, (2005).
[24] P.V. Radovanovic, D.R. Gamilin, Phys.Rev.lett., **91**, 157202 (2003**)**.
[25] S.Deka, P.A. Joy, Chem. Mater., **17**, 6507 (2005**)**.
[26] J.I. Pankove, Optical process in semiconducters., Prentice-Hall: New Jersey, 1971.